Transversal dynamics of a non-locally-coupled map lattice

S. E. de S. Pinto,[1,2] I. L. Caldas,[1] A. M. Batista,[2] S. R. Lopes,[3] and R. L. Viana[3]
[1]*Universidade de São Paulo, 05315-970, São Paulo, SP, Brazil*
[2]*Universidade Estadual de Ponta Grossa, 84032-900, Ponta Grossa, PR, Brazil*
[3]*Universidade Federal do Paraná, 81531-990, Curitiba, PR, Brazil*
(Received 25 September 2006; revised manuscript received 25 April 2007; published 11 July 2007)

A lattice of coupled chaotic dynamical systems may exhibit a completely synchronized state, which defines a low-dimensional invariant manifold in phase space. However, the high dimensionality of the latter typically yields a complex dynamics with many features like chaos suppression, quasiperiodicity, multistability, and intermittency. Such phenomena are described by considering the transversal dynamics to the synchronization manifold for a coupled logistic map lattice with a long-range coupling prescription.

DOI: 10.1103/PhysRevE.76.017202 PACS number(s): 05.45.Ra, 05.45.Jn, 05.45.Xt

Synchronization of chaos in coupled dynamical systems is one of the most intensively investigated dynamical phenomena because of its applications in communications, heartbeat generation, and neural activity [1]. One outstanding feature of the synchronized state of coupled chaotic systems, like maps or continuous-time flows, is that this state lies in a low-dimensional invariant subspace, the synchronization manifold [2]. This greatly simplifies the dynamical behavior of the coupled system, even though its phase space may be high dimensional, allowing stability analysis to be done with the help of a master function [3]. However, besides the completely synchronized states, there is also a plethora of other possible asymptotic states. Such states, although not completely synchronized, may present a variable degree of spatial coherence. In this Brief Report we consider one-dimensional lattices of N coupled chaotic maps, whose transversal dynamics involves $N-1$ degrees of freedom [4]. Among the spatiotemporal features identified in coupled map lattices we find synchronization of chaos [1], pattern formation [5], chaos suppression [6], intermittency [7], and multistability [8]. We will focus on a nonlocal type of coupling for which the interaction between sites decreases with their mutual distances along the lattice in a power-law fashion [9].

Let us consider a general form of a coupled map lattice for a state variable $x_n^{(i)}$ at discrete time n and attached to the site $i=1,2,\ldots,N$:

$$x_{n+1}^{(i)} = \sum_j B_{ij}[f(x_n^{(j)})] = f(x_n^{(i)}) + \sum_j g_{ij} f(x_n^{(j)}), \qquad (1)$$

where the local dynamics is governed by the map $f(x)$, $x\in[0,1]$, and g_{ij} are coupling coefficients. The following necessary and sufficient conditions must hold for all sites i,j such that $x_n^{(i)}$ belong to the interval [0, 1] for all times: $B_{ij}\geq 0$ and $0\leq\Sigma_{j=1}^{N} B_{ij}\leq 1$. We used a nonlocal coupling, for which the (symmetric) coupling coefficients are

$$g_{ij} = \varepsilon[\eta(\alpha)]^{-1}[(1-\delta_{ij})r_{ij}^{-\alpha} - \eta(\alpha)\delta_{ij}], \qquad (2)$$

where $r_{ij}=\min_{\ell\in Z}|i-j+\ell N|$ is the minimum distance between sites i and j; and $\eta(\alpha)=2\Sigma_{r=1}^{N'} r^{-\alpha}$ is the corresponding normalization factor, with $N'=(N-1)/2$ [9]. The parameters $\varepsilon\in[0,1]$ and $\alpha\in[0,\infty)$ represent the strength and effective range of the interactions, respectively. The latter makes it possible to vary the coupling from a global (mean field) [10] to a local (nearest-neighbor) scheme [11] in the limits $\alpha=0$ and $\alpha\to\infty$, respectively, with periodic boundary conditions.

A completely synchronized state ($x_n^{(1)}=x_n^{(2)}=\cdots=x_n^{(N)}$) defines a one-dimensional synchronization manifold $\mathcal{S}$ in N-dimensional phase space. This manifold is invariant if (and only if) $\Sigma_{j=1}^{N} B_{ij}$ is the same for all rows of the matrix B_{ij}. In the specific case of (1) this implies that $\Sigma_{j=1}^{N} g_{ij}=0$, which is fulfilled by the nonlocal prescription (2). All the remaining $N-1$ directions are said to be transversal to $\mathcal{S}$. Since N is usually a large integer, a direct approach to the transversal dynamics is extremely difficult unless we resort to some kind of approximation to reduce the number of degrees of freedom involved, such as computation of the transversal distance to the synchronization manifold, $d_n=\sigma_n\sqrt{N}$, where σ_n is the standard deviation of the state variable values around their spatially averaged value at time n [12]. Thus $d=0$ for a completely synchronized state.

As an additional numerical diagnostic of complete synchronization we consider complex order parameter for the lattice [13]:

$$z_n = R_n e^{2\pi i\varphi_n} \equiv (1/N)\sum_j e^{2\pi i x_n^{(j)}}, \qquad (3)$$

where R_n and φ_n are the amplitude and angle, respectively, of a centroid phase vector (for a one-dimensional chain with periodic boundary conditions). A mean value of the order parameter magnitude, $R_m=\lim_{M\to\infty}(1/M)\Sigma_{n=0}^{M} R_n$, can be computed over a time interval large enough to warrant that the asymptotic state has been achieved by the lattice. A completely synchronized state implies $R_m=1$, whereas nonsynchronized trajectories yield $R_m<1$. Since we found the need of a further indication of the possibly existing attractors outside the synchronization manifold, we also computed the Lyapunov spectrum of the coupled map lattice, so as to obtain the corresponding Lyapunov dimension, which gives a lower bound for the box-counting dimension of the system attractor [14]. If there is a synchronized chaotic attractor in $\mathcal{S}$, it follows that $D>1$ corresponds to nonsynchronized chaotic trajectories.

The dependence of these quantities characterizing transversal dynamics (d, D, and R_m) with the range parameter α,

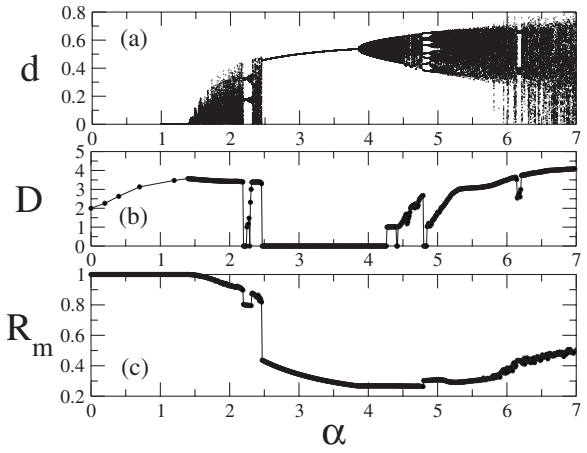

FIG. 1. Bifurcation diagram for (a) d, (b) D, and (c) R_m versus α for $N=5$ and $\varepsilon=1.0$.

keeping the coupling strength fixed at $\varepsilon=1.0$, is illustrated in the bifurcation diagrams depicted in Fig. 1, where we considered a lattice of $N=5$ coupled maps. For $0\leq\alpha<\alpha_c\approx1.388$ the distance to $\mathcal{S}$ is zero [Fig. 1(a)], such that the system only exhibits a completely synchronized state, a fact already expected since we are dealing with global couplings and a large value of ε [7]. The same conclusion comes from Fig. 1(c), where we plot the average order parameter magnitude as a function of α, since $R_m=1$ within this interval. From the corresponding values of the Lyapunov dimension [Fig. 1(b)] we conclude that either the phase space has nonsynchronized attractors coexisting with the synchronized one or the computed values of D reflect a chaotic transient instead of a true attractor. Since Fig. 1(a) was computed using a large number of initial conditions, we favor the latter hypothesis against the former; i.e., the synchronized attractor seems to be unique. However, this does not rule out completely the possibility of having other nonsynchronized attractors, but with extremely small basins of attraction. In fact, a completely synchronized attractor for a coupled lattice of one-dimensional maps would correspond to a dimension of $D=1$ in the thermodynamical limit $N\to\infty$ [12]. The fact that Fig. 1(b) indicates that $2.0\lesssim D\lesssim3.5$ is a consequence of the small lattice size we used.

Nonzero values of d in Fig. 1(a) start to appear only after $\alpha_c\approx1.388$ and, except for a narrow period-2 window at $2.19\lesssim\alpha\lesssim2.32$, the chaotic values of d_n remain so until $\alpha=\alpha_P\approx2.464196$, where a stable fixed-point attractor suddenly appears. According to Fig. 1(c), the corresponding order parameter takes on values lower than 1.0, which is consistent with a loss of spatial coherence due to an intermittent switching between synchronized and nonsynchronized states. Since the synchronization manifold is invariant for our dynamical system, this phenomenon is an example of the so-called *on-off intermittency* [15]. A fixed point for d appears in the parameter interval $\alpha_P<\alpha<\alpha_{NS}\approx3.845$. This does not imply necessarily that we also have a fixed point in the full phase space, but merely that there is probably a low-dimensional attractor for the transversal dynamics. We verified this fact by considering the corresponding Lyapunov dimension [Fig. 1(b)], which vanishes in the same parameter interval for which there is a fixed point for d. This suggests a fixed point of the dynamics in the full phase space, or suppression of chaos. On the other hand, since the mean-order parameter decreases abruptly to values in the range 0.4–0.3 [Fig. 1(c)] this fixed point represents a lattice pattern with low spatial coherence.

Another low-dimensional attractor appears in the period-2 window of the bifurcation diagram of d in Fig. 1(a) at $2.19\lesssim\alpha\lesssim2.32$, which rapidly bifurcates through a subharmonic cascade generating chaotic bands that merge, restoring the chaotic values of d. Since the corresponding Lyapunov dimension is zero therein [Fig. 1(b)], we identify a period-2 nonsynchronized orbit in the full phase space and suppression of chaos takes place here again. For $\alpha_{NS}\approx3.845<\alpha<\alpha_Q\approx4.250$, while the bifurcation diagram indicates that the values of d fill a continuous interval not approaching the synchronization manifold, the Lyapunov dimension remains zero. In this case we have another instance of chaos suppression, but this time yielding a quasiperiodic orbit; i.e., the map iterations densely fill an invariant curve which is the section of a high-dimensional torus. The emergence of such an invariant curve from a fixed point occurs due to a Neimark-Sacker bifurcation at α_{NS}. This quasiperiodic orbit breaks up at α_Q, yielding a chaotic attractor whose dimension increases with α, except for tiny periodic windows in the bifurcation diagram. The chaotic attractor itself is enlarged by an interior crisis at $\alpha=\alpha_{CR}\approx5.8$ and, after that, its dimension achieves a large value ($D=4$ out of a maximum of five dimensions). Moreover, the post-critical trajectories ($\alpha>\alpha_{CR}$) approach the synchronization manifold such that we may have either a high-dimensional chaotic attractor or a extremely long chaotic transient.

After having described qualitatively the transversal dynamics for a wide range of the range parameter, we shall focus on some selected features, which, however, do not exhaust the variety of possible phenomena occurring outside the synchronization manifold for a coupled system.

(i) *Intermittent transition to a synchronized state.* The point α_c in the bifurcation diagram of Fig. 1 marks the transition from a completely synchronized to a nonsynchronized state. In other words, the synchronization manifold $\mathcal{S}$ loses transversal stability such that randomly chosen initial conditions do not generate trajectories which asymptote to $\mathcal{S}$. For $\alpha\gtrsim\alpha_c$ we observe an intermittent switching between synchronized and nonsynchronized behavior, characterized by the alternation of laminar intervals off but near $\mathcal{S}$ with bursting excursions far from $\mathcal{S}$. It is convenient to work with the logarithmic distances to $\mathcal{S}$ defined as $y_n=-\log_{10}(d_n)$, which approach zero with a linear trend $y_n\sim-|\lambda_T|n$, where λ_T is the largest transversal Lyapunov exponent of the system. Useful information on the transversal dynamics can also be drawn from the probability distributions of the logarithmic distances, denoted by $P(y)$, some of them being depicted in Fig. 2 for three values of the difference $\alpha-\alpha_c$. In those cases the numerical results are fitted by an exponential scaling law of the form $P(y)\sim e^{-\gamma y}$ ($\alpha\gtrsim\alpha_c$), where $\gamma=2.182$.

In addition to the linear trend of y_n there are a large number of fractally distributed spikes due to the infinite number of transversely unstable periodic orbits which coexist with the transversely stable orbits embedded in the chaotic syn-

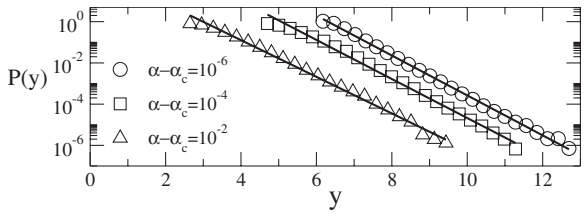

FIG. 2. $P(y)$ for values of α in the vicinity of $\alpha_c \approx 1.388$ for $N=5$ and $\varepsilon=1.0$.

chronized attractor in $\mathcal{S}$ [16]. The involved periodic-orbit structure in $\mathcal{S}$ can be analyzed through computing the finite-time Lyapunov transversal exponent $\tilde{\lambda}_T(n)$. They take on positive (negative) values if the corresponding time-n sections of the trajectory are transversely repelling (attracting) on average with respect to $\mathcal{S}$ [17]. In such cases we compute the probability distribution of the time-n maximal transversal Lyapunov exponent, or $\mathcal{P}(\tilde{\lambda}_T(n))$ [13]. The evolution of the transversal distances from $\mathcal{S}$ can be described by a biased random walk with a reflecting barrier, and the stationary solution of such a stochastic model predicts an exponential dependence for the logarithmic distances just like the one we described, with an exponent $\gamma \equiv 2|\lambda_T|/\sigma^2$, where σ^2 is the variance of the distribution $\mathcal{P}(\tilde{\lambda}_T(n))$ [18]. It turned out that the values predicted by this model agree with those obtained from the least-squares fits in Fig. 2.

(ii) *Type-I intermittent transition preceding suppression of chaos.* A transition from a chaotic to a periodic (fixed point) attractor occurs at $\alpha_P \approx 2.464\,196$ [see Fig. 1(a)]. For $\alpha \lesssim \alpha_P$ there is an intermittent switching between laminar intervals for $d \neq 0$ and bursts, the former being related to stationary but nonsynchronized states of the system [Fig. 3(b)]. The nonsynchronized behavior of the laminar intervals is confirmed by the oscillating behavior of the corresponding order parameter magnitude [Fig. 3(c)]. The laminar intervals have different durations τ_i, and in Fig. 3(a) we plotted the mean laminar duration $\langle\tau\rangle$ versus the parameter distance to the transition point, our numerical results supporting the power-law scaling $\langle\tau\rangle \sim |\alpha-\alpha_P|^{-\beta}$, where $\beta \approx 0.5162$. This value compares well with that predicted by the type-I intermittency for one-dimensional maps [14], suggesting that the essential transversal dynamics is low dimensional.

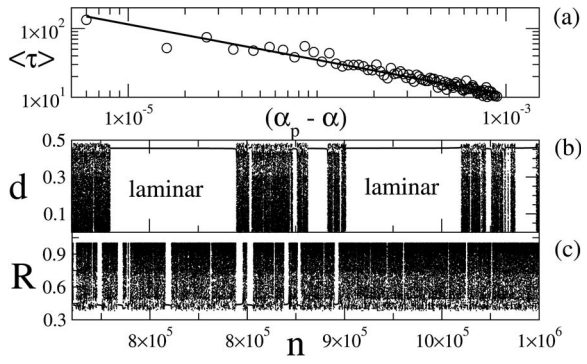

FIG. 3. (a) $\langle\tau\rangle \times (\alpha_p - \alpha)$, where $\alpha_P \approx 2.464196$, with $N=5$ and $\varepsilon=1.0$. Time series of (b) d and (c) R for $\alpha=\alpha_p-10^{-3}$.

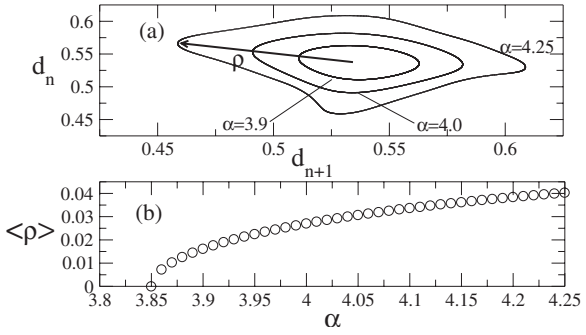

FIG. 4. (a) First return plot for d, with α near $\alpha_{NS} \approx 3.845$, and (b) mean radius $\langle\rho\rangle$ versus α.

(iii) *Neimark-Sacker bifurcation to a high-dimensional torus.* One outstanding feature of the bifurcation diagram [Fig. 1(a)] is the existence of a quasiperiodic orbit for $\alpha_{NS} < \alpha < \alpha_Q$. Some of these orbits are shown Fig. 4(a), where we plot the first return map of d for three values of the α within this interval, yielding invariant curves or two-dimensional sections of a high-dimensional torus outside the synchronization manifold. These curves are topological circles with radius $\rho(d_n)$ and centered at $d_{NS}=0.536\,91$, which is the stable fixed point existing just before a Neimark-Sacker bifurcation occurring at α_{NS}. Just after the bifurcation the radius of the invariant circles increases as $\rho \sim |\alpha-\alpha_{NS}|^{1/2}$ [19], which agrees with the mean radii $\langle\rho\rangle$ of the invariant curves we have numerically determined [Fig. 4(b)].

(iv) *Multistability in periodic windows.* There is an involved periodic window in the interval $\alpha \in [4.4, 5.1]$ of Fig. 1(a) within the one-band chaotic attractor evolving from the quasiperiodic orbit breakup at α_Q and which we magnify in Figs. 5(a) and 5(b). Moreover, while the former was generated using a new set of initial conditions for each value of α considered, the latter was plotted using, as initial conditions for a given value of α, the final points of the trajectory obtained for the previous value of α. As a result, while in Fig. 5(a) we sample a larger fraction of the phase space and find a large number of coexisting periodic and chaotic attractors, in Fig. 5(b) we isolate a single period-4 orbit which subsequently evolves through a period-doubling cascade to chaos.

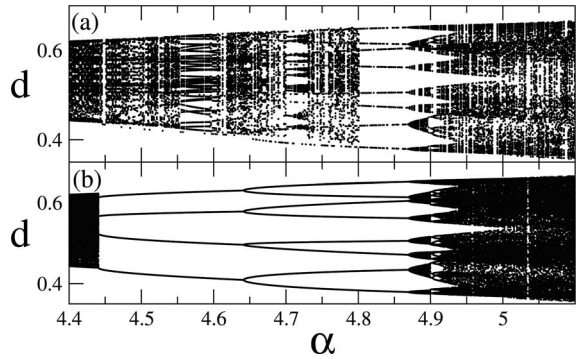

FIG. 5. Periodic window in the bifurcation diagram of Fig. 1 using (a) new sets of initial conditions for each α value and (b) the final state for a given α-value as the initial condition for the next α.

This is a single example of the richness of the behavior observed in the transversal dynamics.

In conclusion, we described in this Brief Report a view of the complexity present in the nonsynchronized dynamics of a coupled chaotic system, focusing on the transversal directions to the synchronized manifold. The Lyapunov spectrum of the system is used in two ways. First, it gives a lower bound on the dimension of the transversal dynamics attractor by means of the Lyapunov dimension. The second is the maximum transversal exponent, in both its infinite- and finite-time versions. While the former is important to describe the overall approach to the synchronized state, the latter can be used to characterize statistically the distribution of the logarithmic distances to the synchronization manifold. These facts are not limited to the special coupled map lattice we have chosen, but can be useful in any coupled chain of maps or oscillators. For the specific system we investigated, we were able to describe qualitatively and quantitatively the dynamics after the loss of transversal stability of the synchronized state. In particular, the distribution we found of the logarithmic distances to the synchronization manifold gives results in agreement with a general stochastic model and the intermittency related to a transition to chaos suppression loss presents features of the type-I Pomeau-Manneville scenario. These features suggest that there are low-dimensional features of the transversal dynamics which can be explored by means of indicators like those used in this work, constituting ways to explore the richness of the dynamics of high-dimensional systems.

This work was partially supported by FAPESP, CAPES, CNPq and Fundação Araucária (Paraná).

[1] A. Pikovsky, M. Rosemblum, and J. Kurths, *Synchronization: A Universal Concept in Nonlinear Sciences* (Cambridge University Press, Cambridge, England, 2001); S. Boccaletti, J. Kurths, G. Osipov, D. L. Valladares, and C. S. Zhou, Phys. Rep. **366**, 1 (2002); *Synchronization: Theory and Applications*, edited by A. Pikovsky and Yu. Maistrenko (Kluwer, Dordrecht, 2003).

[2] L. M. Pecora, T. L. Carroll, G. A. Johnson, D. J. Mar, and G. F. Heagy, Chaos **7**, 520 (1997).

[3] L. M. Pecora and T. L. Carroll, Phys. Rev. Lett. **80**, 2109 (1998).

[4] *Theory and Applications of Coupled Map Lattices*, edited by K. Kaneko (Wiley, Chichester, 1993).

[5] T. Shibata and K. Kaneko, Physica D **181**, 197 (2003); P. G. Lind, J. Corte-Real, and J. A. C. Gallas, Phys. Rev. E **69**, 066206 (2004).

[6] P. Parmananda, M. Hildebrand, and M. Eiswirth, Phys. Rev. E **56**, 239 (1997); P. M. Gade, *ibid.* **57**, 7309 (1998).

[7] R. L. Viana, C. Grebogi, S. E. de S. Pinto, S. R. Lopes, A. M. Batista, and J. Kurths, Phys. Rev. E **68**, 067204 (2003).

[8] A. Lemaitre and H. Chaté, Phys. Rev. Lett. **82**, 1140 (1999).

[9] A. Torcini and S. Lepri, Phys. Rev. E **55**, R3805 (1997); R. L. Viana and A. M. Batista, Chaos, Solitons Fractals **9**, 1931 (1998); S. E. de S. Pinto and R. L. Viana, Phys. Rev. E **61**, 5154 (2000).

[10] K. Kaneko, Physica D **41**, 137 (1990); Y. Kuramoto and H. Nakao, Physica D **103**, 294 (1997); P. M. Gade and C.-K. Hu, Phys. Rev. E **60**, 4966 (1999).

[11] S. Sinha, D. Biswas, M. Azam, and S. V. Lawande, Phys. Rev. A **46**, 6242 (1992).

[12] S. E. de Souza Pinto, J. T. Lunardi, A. M. Saleh, and A. M. Batista, Phys. Rev. E **72**, 037206 (2005).

[13] R. L. Viana, C. Grebogi, S. E. de S. Pinto, S. R. Lopes, A. M. Batista, and J. Kurths, Physica D **206**, 94 (2005).

[14] E. Ott, *Chaos in Dynamical Systems*, 2nd ed. (Cambridge University Press, Cambridge, England, 2001).

[15] M. Ding and W. Yang, Phys. Rev. E **56**, 4009 (1997).

[16] P. Ashwin, J. Buescu, and I. Stewart, Nonlinearity **9**, 703 (1996); C. Anteneodo, S. E. de S. Pinto, A. M. Batista, and R. L. Viana, Phys. Rev. E **68**, 045202(R) (2003).

[17] The largest transversal exponent is the infinite-time limit of the time-n exponents: $\lambda_T = \lim_{n\to\infty} \tilde{\lambda}_T(n)$.

[18] T. Sauer, C. Grebogi, and J. A. Yorke, Phys. Rev. Lett. **79**, 59 (1997); R. L. Viana, S. E. de S. Pinto, and C. Grebogi, Phys. Rev. E **66**, 046213 (2002).

[19] S. Wiggins, *Introduction to Applied Nonlinear Dynamical Systems and Chaos* (Springer-Verlag, New York, 1990).